J1.1 THE GOCART MODEL STUDY OF AEROSOL COMPOSITION AND RADIATIVE FORCING

Mian Chin[1,2 *], Paul Ginoux[1,2], Brent Holben[2], Ming-Dah Chou[2], Stefan Kinne[2,3], Clark Weaver[2,4]

[1]Georgia Institute of Technology, Atlanta, Georgia
[2]NASA Goddard Space Flight Center, Greenbelt, Maryland
[3]University of Maryland at Baltimore County, Baltimore, Maryland
[4]Emergent Inc., Maryland

1. INTRODUCTION

Aerosols affect the climate directly by absorbing or scattering radiation, and indirectly by altering cloud formation and cloud properties. It is projected that economic development in the next century could lead to a significant increase in aerosol and its precursor emissions. However, the magnitudes of the anthropogenic aerosol forcing is poorly constrained, because we have limited knowledge of the processes that control aerosol distributions and the relationships that exist between the aerosol mass and their optical properties. It is still unclear how the climate will respond to the rapid economic and population growth in developing countries and to the reduction of aerosol precursor emissions in some developed countries in the next century.

Here we present a global model assessment of aerosol composition, optical thicknesses, and radiative forcing in the present day and in the next century using the emission scenarios projected by the Intergovernment Panel on Climate Change (IPCC). Five major tropospheric aerosols, including sulfate, organic carbon, black carbon, dust, and sea-salt, are simulated in the Georgia Tech/Goddard Ozone Chemistry Aerosol Radiation and Transport (GOCART) model (Chin et al., 2000a; Ginoux et al., 2000). In this presentation we compare model simulated aerosol optical thicknesses for the present time with the ground-based measurements, estimate radiative forcing by individual aerosol types, and assess the atmospheric response to the IPCC projected anthropogenic emission scenarios for years 2000, 2030 and 2100.

2. THE GOCART MODEL

2.1 General

The GOCART model is a global scale model driven by the Goddard Earth Observing System Data Assimilation System (GEOS DAS). It has a horizontal resolution of 2° latitude by 2.5° longitude and 20 to 40 vertical layers (vertical resolution depends on the version of GEOS DAS). The model contains the following modules in aerosol simulation: emission, which includes sulfur, dust, black carbon and organic carbon, and sea-salt emissions; chemistry, which includes in-air and in-cloud oxidations of sulfate precursors (SO_2 and DMS); advection, which is computed by a flux-form semi-Lagrangian method; boundary layer turbulent mixing, which uses a second-order closure scheme; moist convection, which is calculated using archived cloud mass flux fields; dry deposition, which uses a resistance-in-series algorithm as a function of surface type and meteorological conditions; and wet deposition, which accounts for the scavenging of soluble species in convective updrafts and rainout/washout in large-scale precipitation. More detailed description and references are given in Chin et al. (2000a) and Ginoux et al. (2000).

2.2 Size Distributions

We consider seven size bins for dust (r_{eff} =0.1-0.18, 0.18-0.3, 0.3-0.6, 0.6-1, 1-1.8, 1.8-3, 3-6 μm) and four size bins for dry sea-salt (r_{eff} =0.1-0.5, 0.5-1.5, 1.5-5, 5-10 μm). We assume lognormal size distributions for sulfate (dry r_{eff} = 0.24 μm), organic carbon (dry r_{eff} = 0.10 μm), and black carbon (dry r_{eff} = 0.04 μm) aerosols. We also assume lognormal distributions for each dust and sea-salt bins. With the exception of dust, aerosols are considered to be hydrophilic, i.e., their size increases with the increase of ambient relative humidity. Table 1 lists the effective radius of several types of aerosols at different ambient relative humidities in our model, based on the Global Aerosol Data Base (Köpke et al., 1997).

Table 1. Effective radius (μm) of the hydrophilic aerosols[†]

RH(%)	0	50	70	80	90	95	99
SO4	0.235	0.333	0.369	0.399	0.457	0.534	0.781
OC	0.100	0.124	0.135	0.145	0.165	0.189	0.253
BC	0.039	0.039	0.041	0.047	0.055	0.061	0.074
SSa	0.798	1.283	1.444	1.589	1.899	2.311	3.801
SSc	5.73	9.24	10.39	11.44	13.70	16.75	28.15

[†]SO4, sulfate; OC, organic carbon; BC, black carbon; SSa, accumulation mode sea-salt; SSc, coarse mode sea-salt.

2.3 Radiative Properties

The radiative properties include the extinction coefficient (Q), single scattering albedo (ω_0), and asymmetry factor (g). These properties, which are size and wavelength dependent, have been calculated using the Mie theory with the refractive indices from Köpke et al. (1997)

**Corresponding author address*: Mian Chin, NASA Goddard Space Flight Center, Code 916, Greenbelt, MD 20771; e-mail: chin@rondo.gsfc.nasa.gov.

and the size distributions described above. For hydrophilic aerosols the effective refractive indices are obtained by volume weighing of the dry aerosol and water. Table 2 lists the values of Q, ω_0, and g at 550 nm for each aerosol type at 7 different size groups. For hydrophilic aerosols, the size groups correspond to the radius at 7 different relative humidities in Table 1. For dust aerosol, the size groups are given at the beginning of section 2.2.

Table 2. Optical parameters at 550 nm for 7 size groups[†]

Size		1	2	3	4	5	6	7
SO4	Q	1.678	1.984	2.096	2.186	2.314	2.455	2.670
	ω_0	1.000	1.000	1.000	1.000	1.000	1.000	1.000
	g	0.716	0.768	0.779	0.784	0.791	0.797	0.798
OC	Q	0.675	0.725	0.765	0.863	0.901	1.025	1.358
	ω_0	0.961	0.976	0.981	0.984	0.989	0.993	0.997
	g	0.605	0.663	0.682	0.697	0.718	0.738	0.766
BC	Q	0.487	0.487	0.474	0.419	0.364	0.345	0.335
	ω_0	0.209	0.209	0.214	0.248	0.323	0.383	0.537
	g	0.337	0.337	0.350	0.405	0.470	0.504	0.567
SSa	Q	2.699	2.547	2.544	2.508	2.444	2.362	2.221
	ω_0	1.000	1.000	1.000	1.000	1.000	1.000	1.000
	g	0.695	0.774	0.774	0.785	0.794	0.799	0.824
SSc	Q	2.159	2.115	2.117	2.123	2.086	2.073	2.063
	ω_0	1.000	1.000	1.000	1.000	1.000	1.000	1.000
	g	0.790	0.841	0.850	0.852	0.858	0.865	0.872
Dust	Q	1.139	2.058	2.736	2.706	2.464	2.297	2.189
	ω_0	0.968	0.965	0.951	0.920	0.872	0.811	0.731
	g	0.631	0.669	0.688	0.702	0.743	0.795	0.851

[†]SO4, sulfate; OC, organic carbon; BC, black carbon; SSa, accumulation mode sea-salt; SSc, coarse mode sea-salt.

3. RESULTS

We present here the results from our standard model simulation for 1990 assuming that these results are typical for a "normal" year, i.e., without major anomalies such as large volcanic eruption. The anthropogenic emission of sulfur is taken from the Emission Database for Global Atmospheric Research (EDGAR) for 1990. Other sulfur emissions include biomass burning and volcanic emissions of SO_2 and oceanic emissions of DMS (Chin et al., 2000a), Organic and black carbon emissions include anthropogenic and biomass burning emissions (Cooke et al., 1996, 1999; Liousse et al., 1996) as well as emissions of natural volatile organic carbon (Guenther et al., 1995). Dust emission is parameterized as a function of surface topography, soil type, surface wind speed and wetness (Ginoux et al., 2000). Sea-salt emission is calculated as a function of wind speed (Monahan et al., 1986). Detailed description of sulfur and dust models and comparison of atmospheric concentrations with observations are given in Chin et al. (2000a, b) and Ginoux et al. (2000). We show here the model calculated aerosol optical thicknesses (AOT) and the estimated direct radiative forcing by aerosols.

3.1 Aerosol Optical Thickness (AOT)

The AOTs are calculated as follows. For each aerosol type or size i at a given wavelength, the optical thickness τ_i is

$$\tau_i = (3Q_iM_i) / (4\rho_i r_i)$$

where Q_i is the extinction coefficient, M_i is the mass loading, ρ_i is the density, and r_i is the effective radius.

Figure 1 shows the seasonally and annually averaged total aerosol optical thicknesses at 550 nm from our standard simulations for 1990. Globally, the averaged AOT at 550 nm in 1990 is 0.035 for sulfate, 0.010 for organic carbon, 0.0043 for black carbon, 0.057 for dust, and 0.027 for sea-salt. AOT for carbonaceous aerosol in Figure 1 includes both organic carbon and black carbon. Although the AOT of black carbon is relatively thin, black carbon plays an important role in determining the total aerosol rediative forcing, as we will discuss in the next section. Sulfate aerosol is mainly concentrated in three major pollution regions: eastern North America, Europe, and eastern Asia. Carbonaceous aerosols are optically the most important aerosol over the equatorial South America and Africa mainly over the biomass burning regions. Dust aerosol dominates the total AOT in latitudinal band of 10° S-40° N over the Atlantic and Indian oceans as well as over the source regions of northern Africa, Asia, and Australia. In the southern hemisphere, sea-salt is the major type of aerosol at latitudes higher than 30° S where it contributes 40-80% to the total AOT.

The AOT calculated in the model are compared with those measured from the sun-photometers in the Aerosol Robotic Network (AERONET) (Holben et al., 2000). Figure 2 shows the comparison at 8 AERONET sites. The model agrees with the observations relatively well at Cape Verde, Bermuda, Barbados, and Ispra. Discrepancies exist at other sites, which are directly related to the emission and wet removal processes in the model. For example, the comparisons at Banizonmbou and Mongu clearly point to the problems in biomass burning emission intensities and seasonality, and the comparison at Lanai indicates that the dust loading is too high over the North Pacific, probably a result of overestimating small particle emission from Asian desert (Ginoux et al., 2000).

3.2 *Direct Shortwave Radiative Forcing by Aerosols*

The calculations of radiative forcing are carried out in a radiative transfer model at NASA Goddard Climate and Radiation Branch (Chou and Suarez, 1999). The shortwave radiative processes in the model are parameterized in 11 spectral bands (0.2-10 μm) accounting for the absorption by O_3, O_2, CO_2, H_2O and scatterubg by gas and particles. To estimate the radiative effect of specific type of aerosos, the shortwave flux was first computed without aerosols in the atmosphere, and then computed with a specific type of aerosol distributions obtained from the GOCART model. The difference in the flux between

the runs with and without aerosol is referred to as the instantaneous radiative forcing. We assume here only external mixture of different types of aerosols.

Figure 3 shows the zonally and annually averaged direct shortwave (λ < 10 μm) forcing by different types of aerosols at the top of the atmosphere (TOA). Globally, all the aerosols cause negative radiative forcing in the shorwave spectral region except black carbon. Dust exerts the most negative forcing (-1.4 W m^{-2}), followed by sulfate (-1.0 W m^{-2}), sea-salt (-0.5 W m^{-2}), and organic carbon (-0.3 W m^{-2}). In contrast, black carbon is highly absorbing with an average forcing of +0.4 W m^{-2} at TOA. The magnitude of forcing by black carbon is higher than that of organic carbon (with opposit sign) even though at 550 nm the AOT of black carbon is only less than half of that of organic carbon.

4. SIMULATIONS OF FUTURE EMISSION SCENARIOS

To estimate the aerosol climate forcing in response to the future economic development and human activities, we use the projected anthropogenic emission data sets for years 2000, 2030, and 2100 from the Special Report on Emissions Scenarios (SRES) developed for the IPCC (Nakicenovic et al., 1999). Emissions of sulfur and carbon from natural sources are based on the data set used in the IPCC model intercomparison workshop (Penner et al., 2000). Dust and sea-salt emissions are kept the same as in our standard simulations. Emission source strengths in our standard run for 1990 (STD) and in 4 IPCC assessment scenarios (SC1 - SC4) are given in Table 3. Note that SO_2 from biomass burning and sporadically erupting volcanoes are not included in the IPCC emission scenarios.

Table 3. Global Emission Scenarios. Sulfur: TgS yr^{-1}; OC: TgOM yr^{-1}; BC: TgC yr^{-1}; Dust: Tg yr^{-1}; Sea-salt: Tg yr^{-1}.

Scenario		STD	SC1	SC2	SC3	SC4
Year		1990	2000	2030	2100	2100
Sulfur†	A	72.8	69.0	111.9	60.3	28.6
	N	13.3	25.3	25.3	25.3	25.3
	V	5.5	4.8	4.8	4.8	4.8
	B	2.3				
OC†	A+B	73.2	81.4	108.6	189.5	75.6
	N	12.7	12.7	12.7	12.7	12.7
BC†	A+B	12.4	12.4	16.2	28.8	12.0
Dust		1830	1830	1830	1830	1830
Sea-Salt		5820	5820	5820	5820	5820

†A: anthropogenic; B: biomass burning; N: natural; V: volcanic

We have done the same calculations using the projected future emission scenarios as in our standard model setup. Shown in Figure 4 are the atmospheric burden, optical thickness at 550 nm, and shortwave radiative forcing versus the different emission rates in the standard run and in the IPCC future scenarios. It is remarkable that globally the atmospheric burden, aerosol optical thickness, and radiative effects almost linearly respond to the total emission. If the slopes in Figure 4 are used to estimate the atmospheric response to the changes of future emissions, then for every Tg change of annual emissions of sulfur, organic matter, and black carbon, the direct radiative forcing at TOA could change -0.012, -0.004, and +0.027 W m^{-2}, respectively. Although the linear relationships are not expected to hold at seasonal and regional scales and the calculations are simplified as they do not take into account of the complex mixing state of aerosols, the results in Figure 4 clearly indicate that emission control is the fundamental and the most important step in reducing the anthropogenic aerosol climate forcing.

REFERENCES

Chin, M., R. B. Rood, S.-J. Lin, J.-F. Müller, and A. M. Thompson, 2000a: Atmospheric sulfur cycle simulated in the global model GOCART: Model description and global properites. *J. Geophys. Res., 105*, 24,671-24,687.

Chin, M., D. L. Savoie, B. J. Huebert, A. R. Bandy, D. C. Thorton, T. S. Bates, P. K. Quinn, E. S. Saltzman, and W. J. De Bruyn, 2000b: Atmospheric sulfur cycle simulated in the global model GOCART: Comparison with field observations and regional budgets. *J. Geophys. Res., 105*, 24,689-24,712.

Chou, M.-D. and M. J. Suarez, 1999: A solar radiation parameterization for atmospheric studies, *NASA/TM-1999-104606, Vol. 15*.

Cooke, W. F. and J. J. N. Wilson, 1996: A global Black carbon aerosol model. *J. Geophys. Res., 101,* 19,393-19,409.

Cooke, W. F., C. Liousse, H. Cachier, and J. Feichter, 1999: Construction of a 1° x1° fossil fuel emission data set for carbonaceous aerosol and implimentation and radiative impact in the ECHAM4 model. *J. Geophys. Res., 104,* 22,137-22,162.

Ginoux, P., M. Chin, I. Tegen, J. Prospero., B. Holben, O. Dubovik, and S.-J. Lin, 2000: Sources and distributions of dust aerosols simulated with the GOCART model. submitted to *J. Geophys. Res.*

Guenther, A., et al., 1995: A global model of natural volatile organic compound emissions. *J. Geophys. Res., 100,* 8873-8892.

Holben, B. N., et al., 2000: An emerging ground-based aerosol climatology: Aerosol optical depth from AERONET, submitted to *J. Geophys. Res.*

Köpke, P., M. Jess, I. Schult, and E. P. Shettle, 1997: Global Aerosol Data Set, Report No. 243, Max-Planck Institut für Meteorologie.

Liousse, C., J. E. Penner, C. Chuang, J. J. Walton, H. Eddleman, and H. Cachier, 1996: A global three-dimensional model study of carbonaceous aerosols. *J. Geophys. Res., 101,* 19,411-19,432.

Monanhan, E. C., D. E. Spiel, and K. L. Davidson, 1986: A model of marine aerosol generation via whitecaps and wave disruption in oceanic whitecaps, in *Oceanic whiitecaps and their role in air-sea exchange processes*, E. C. Monahan and G. M. Niocaill (eds), D. Reidel Publishing, Dordrecht, Holland, pp. 167-174.

Nakicenovic, N., et al., 2000: Special Report on Emissions Scenarios. IPCC Working Group III Report.

Penner, J. E. et al., 2000: Aerosols, their Direct and Indirect Effects, IPCC Working Group I Third Assessment Report.

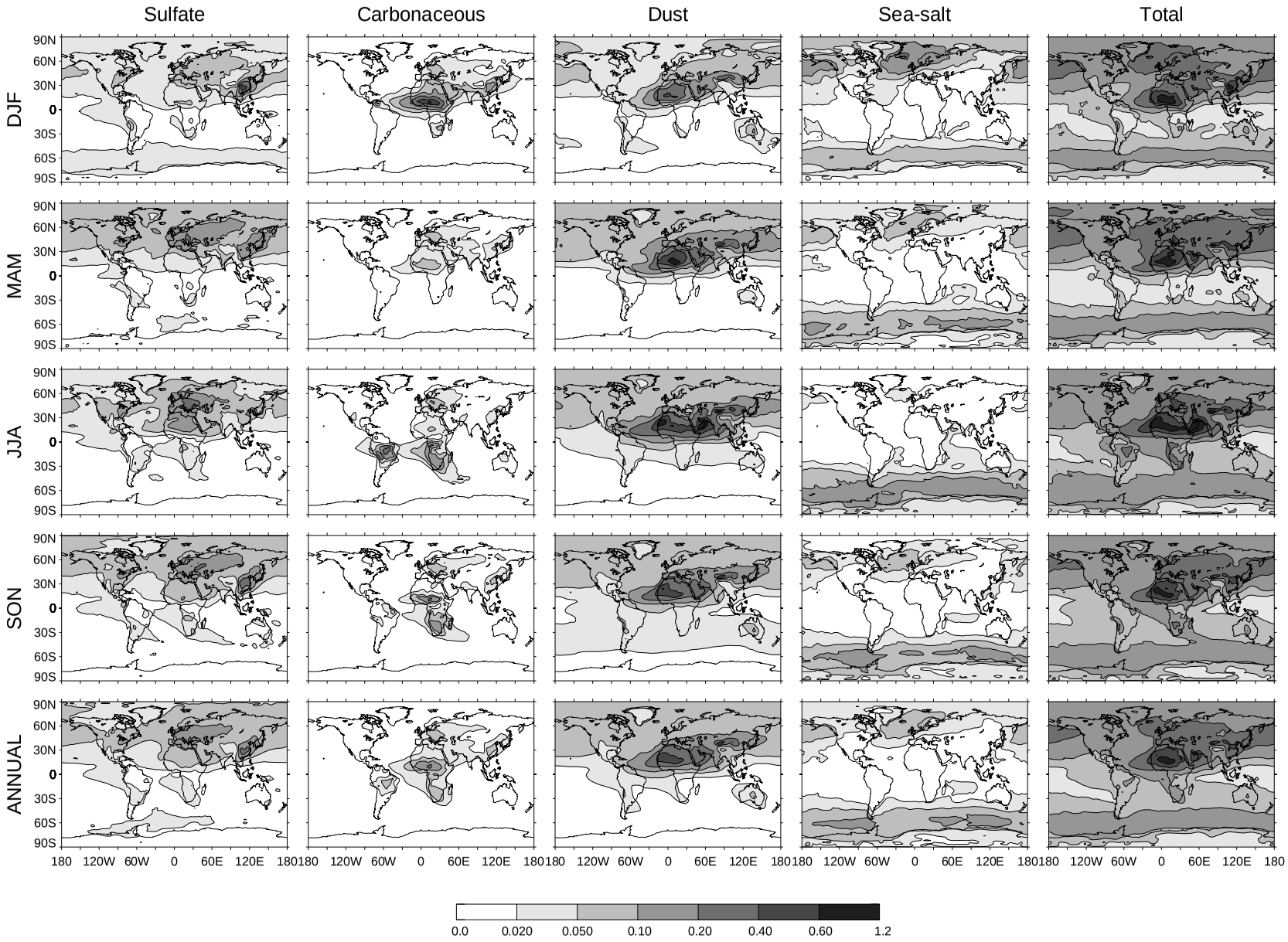

Figure 1. Calculated seasonally and annually averaged aerosol optical thicknesses at 550 nm in 1990.

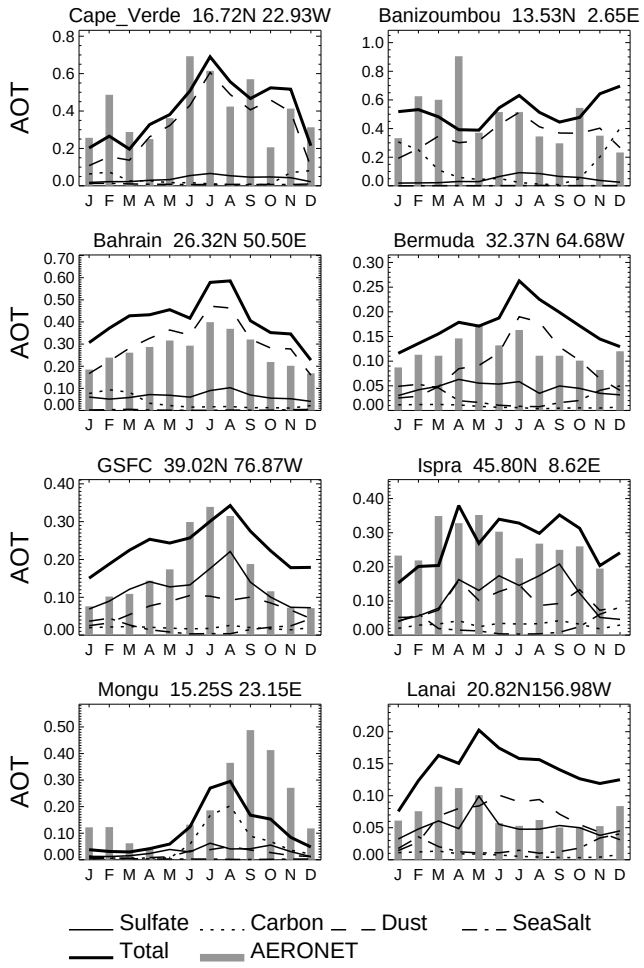

Figure 2. Comparison of calculated AOT at 500 nm (lines) with AERONET measurements (vertical bars). Names and locations of the sites are indicated at the top. Model results are for 1996. AERONET data are from 1993-1999, with diffferent period for each site [Holben et al., 2000].

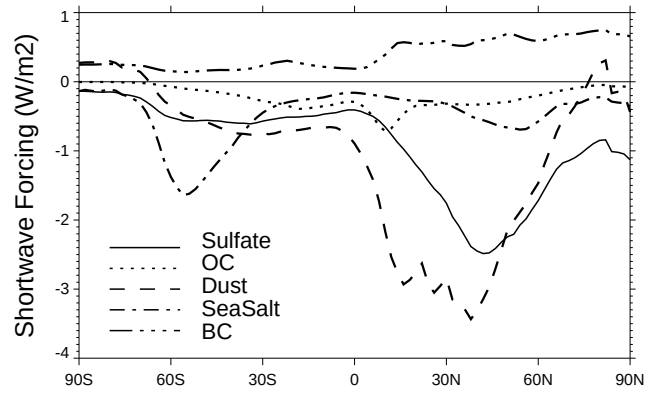

Figure 3. Zonally averaged aerosol shortwave radiative forcing at the top of the atmosphere.

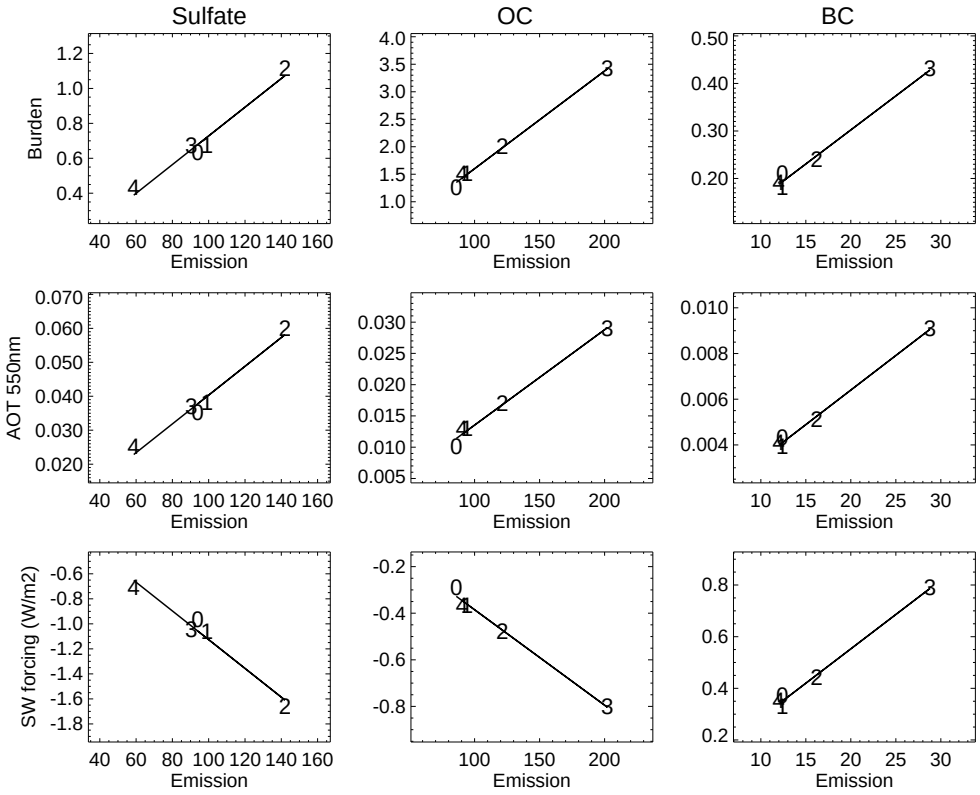

Figure 4. Model calculated atmospheric aerosol burden, 550 nm optical thickness, and shortwave radiative forcing for different emission scenarios (0=STD, 1=SC1, 2=SC2, 3=SC3, 4=SC4).